nature geoscience

ARTICLES

https://doi.org/10.1038/s41561-021-00726-z

Control of particulate nitrate air pollution in China

Shixian Zhai[1], Daniel J. Jacob[1]✉, Xuan Wang[2], Zirui Liu[3], Tianxue Wen[3], Viral Shah[1], Ke Li[1], Jonathan M. Moch[1], Kelvin H. Bates[1], Shaojie Song[1], Lu Shen[1], Yuzhong Zhang[4,5], Gan Luo[6], Fangqun Yu[6], Yele Sun[3], Litao Wang[7], Mengyao Qi[7], Jun Tao[8], Ke Gui[9], Honghui Xu[10], Qiang Zhang[11], Tianliang Zhao[12], Yuesi Wang[3], Hyun Chul Lee[13], Hyoungwoo Choi[13] and Hong Liao[14]

The concentration of fine particulate matter ($PM_{2.5}$) across China has decreased by 30–50% over the period 2013–2018 due to stringent emission controls. However, the nitrate component of $PM_{2.5}$ has not responded effectively to decreasing emissions of nitrogen oxides and has actually increased during winter haze pollution events in the North China Plain. Here, we show that the GEOS-Chem atmospheric chemistry model successfully simulates the nitrate concentrations and trends. We find that winter mean nitrate would have increased over 2013–2018 were it not for favourable meteorology. The principal cause of this nitrate increase is weaker deposition. The fraction of total inorganic nitrate as particulate nitrate instead of gaseous nitric acid over the North China Plain in winter increased from 90% in 2013 to 98% in 2017, as emissions of nitrogen oxides and sulfur dioxide decreased while ammonia emissions remained high. This small increase in the particulate fraction greatly slows down deposition of total inorganic nitrate and hence drives the particulate nitrate increase. Our results suggest that decreasing ammonia emissions would decrease particulate nitrate by driving faster deposition of total inorganic nitrate. Decreasing nitrogen oxide emissions is less effective because it drives faster oxidation of nitrogen oxides and slower deposition of total inorganic nitrate.

The Clean Air Action of the Chinese government, initiated in 2013, has imposed increasingly stringent emission controls to decrease fine particulate matter pollution ($PM_{2.5}$, particles smaller than 2.5 μm in diameter)[1]. Observations from the China Ministry of Ecology and Environment (MEE) monitoring network show a 30–50% decrease in annual mean $PM_{2.5}$ across the country from 2013 to 2018 that can be largely credited to emission controls[2,3]. However, the nitrate (NO_3^-) component of $PM_{2.5}$ has not shown a consistent decrease[4,5], despite an estimated 21% nationwide reduction in the emissions of nitrogen oxides ($NO_x \equiv NO + NO_2$) from fuel combustion[6]. Wintertime nitrate in Beijing has shown no decrease[5,7–9], despite a 43% reduction in NO_x emissions[10], and has in fact increased during the severe pollution events known as winter haze[11–13]. Nitrate is now the principal component of Beijing winter haze pollution, contributing to 30–40% of $PM_{2.5}$ mass during winter haze days in 2016–2019[11–16]. There is an urgent need to better understand why nitrate is not decreasing.

Particulate nitrate originates from the atmospheric oxidation of NO_x to nitric acid (HNO_3), which then partitions into the particulate phase depending on the availability of ammonia (NH_3) as well as temperature and relative humidity. NH_3 is mainly emitted by agriculture, but vehicles may also be an important factor in urban environments[17–20]. As a base, NH_3 first neutralizes sulfate, and the remaining NH_3 can then form particulate ammonium nitrate (NH_4NO_3) in equilibrium with the gas phase. The simplest explanation for the lack of nitrate response to NO_x emission decreases would be limitation by NH_3, combined with strong SO_2 emission controls under the Clean Air Action allowing more NH_3 to be available to form nitrate. However, this is not the case over North China, because NH_3 emissions are very high, so NH_4NO_3 formation is not limited by the supply of NH_3 but instead by that of total nitrate ($NO_3^T \equiv HNO_3 + NO_3^-$)[13,21,22]. Satellite observations show an increase of NH_3 over eastern China from 2013 to 2017, attributed to the decrease in sulfate[4,23,24].

Another possible explanation for the lack of nitrate decrease would be faster conversion of NO_x to NO_3^T due to an increase in oxidants[9,25]. The conversion takes place in the daytime by gas-phase oxidation of NO_2 by the hydroxyl radical (OH). At night it takes place by oxidation of NO_2 by ozone (O_3) to produce the NO_3 radical, which combines with NO_2 to form N_2O_5, which then hydrolyses to nitrate in aqueous particles. Additional pathways include uptake of NO_2 and NO_3 in aqueous particles and oxidation of volatile organic compounds (VOCs) by the NO_3 radical[25–28]. Decreasing NO_x emissions in winter would drive an increase in ozone and OH, shortening

[1]John A. Paulson School of Engineering and Applied Sciences, Harvard University, Cambridge, MA, USA. [2]School of Energy and Environment, City University of Hong Kong, Hong Kong SAR, China. [3]State Key Laboratory of Atmospheric Boundary Layer Physics and Atmospheric Chemistry, Institute of Atmospheric Physics, Chinese Academy of Sciences, Beijing, China. [4]Key Laboratory of Coastal Environment and Resources of Zhejiang Province (KLaCER), School of Engineering, Westlake University, Hangzhou, Zhejiang, China. [5]Institute of Advanced Technology, Westlake Institute for Advanced Study, Hangzhou, Zhejiang, China. [6]Atmospheric Sciences Research Center, University at Albany, Albany, NY, USA. [7]College of Energy and Environmental Engineering, Hebei University of Engineering, Handan, China. [8]Institute for Environmental and Climate Research, Jinan University, Guangzhou, China. [9]Key Laboratory for Atmospheric Chemistry, Chinese Academy of Meteorological Sciences, Beijing, China. [10]Zhejiang Institute of Meteorological Sciences, Hangzhou, China. [11]Department of Earth System Science, Tsinghua University, Beijing, China. [12]Key Laboratory for Aerosol-Cloud-Precipitation of China Meteorological Administration, Collaborative Innovation Center on Forecast and Evaluation of Meteorological Disasters, School of Atmospheric Physics, Nanjing University of Information Science and Technology, Nanjing, China. [13]Samsung Advanced Institute of Technology, Suwon-si, Gyeonggi-do, Republic of Korea. [14]Jiangsu Key Laboratory of Atmospheric Environment Monitoring and Pollution Control, Collaborative Innovation Center of Atmospheric Environment and Equipment Technology, School of Environmental Science and Engineering, Nanjing University of Information Science and Technology, Nanjing, China. ✉e-mail: djacob@fas.harvard.edu

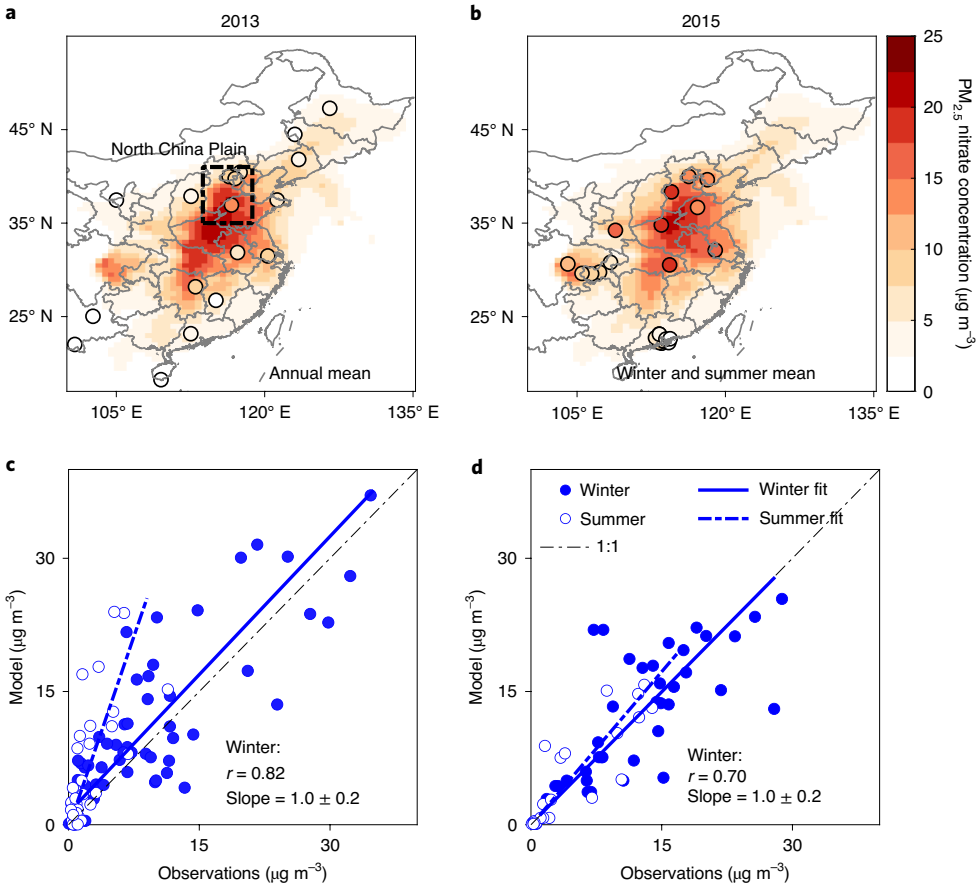

Fig. 1 | $PM_{2.5}$ nitrate concentrations in China and comparisons between observations and GEOS-Chem model results. a,**b**, Surface air $PM_{2.5}$ nitrate concentrations from two nationwide datasets (circles) and GEOS-Chem (background) for 2013 (**a**, annual mean) and 2015 (**b**, summer and winter mean). The colour bar shows $PM_{2.5}$ nitrate concentration in μg m^{-3}. **c**,**d**, Scatterplots of observed and modelled winter (filled circles) and summer (open circles) monthly mean (seasonal mean for the 2015 dataset) nitrate at individual sites. Also shown in **c** and **d** are the 1:1 lines, the wintertime correlation coefficients (*r*) between model and observations, and the corresponding reduced-major-axis regressions and slopes (±95% confidence interval). The 2013 dataset is from the Campaign on Atmospheric Aerosol Research network of China (CARE-China), with nitrate measured by ion chromatography[36,48]. The 2015 dataset is from ref. [37], and only includes sites that have both winter and summer observations. The dashed rectangle in **a** delineates the North China Plain region as defined in this paper (113.75°–118.75° E, 35°–41° N).

the NO_x lifetime against conversion to NO_3^T (refs. [9,25]). Satellite data and GEOS-Chem model simulations for China suggest that the lifetime of NO_x against conversion to NO_3^T has decreased in winter, although not enough to overcome the effect of decreasing NO_x emissions[25]. Decreasing VOC emissions would be beneficial by decreasing oxidant levels and hence increasing the NO_x lifetime[29,30], but a model simulation with 30% reduction of VOC emissions together with 32% reduction of NO_x emissions for 2010–2017 finds only an 8.6% decrease in wintertime nitrate in northern China[9].

In this Article, we aim to understand the factors controlling $PM_{2.5}$ nitrate in China by interpreting observed nitrate trends for 2013–2018 with the GEOS-Chem atmospheric chemistry model, driven by the Multi-resolution Emission Inventory for China (MEIC)[6]. GEOS-Chem has been extensively evaluated with observations of $PM_{2.5}$, NO_x and oxidant chemistry in China[25,31–33]. Here, we implement a new GEOS-Chem wet scavenging scheme by ref. [34] that corrects previous overestimates of $PM_{2.5}$ nitrate and reproduces the observed nitrate wet deposition fluxes from the National Nitrogen Deposition Monitoring Network (NNDMN[35]; Extended Data Fig. 1). We find in the model that the major cause for the lack of response of nitrate to NO_x emission controls in winter, including the increase of nitrate during winter haze episodes, is a large increase in the NO_3^T lifetime against deposition driven by a relatively small increase in the particulate fraction of NO_3^T. From there we suggest that NH_3 emission controls would be most effective for decreasing $PM_{2.5}$ nitrate.

Particulate nitrate distributions and trends

Extensive data for total $PM_{2.5}$ in China are available from the MEE network[2], but data for $PM_{2.5}$ components are limited to research sites that are generally operated only for brief periods. Figure 1 compares GEOS-Chem model results to $PM_{2.5}$ nitrate concentrations in two nationwide observational datasets for 2013 and 2015[36,37]. Additional comparisons for the ensemble of $PM_{2.5}$ components are shown in Extended Data Figs. 2 and 3. Annual mean $PM_{2.5}$ nitrate in eastern China can reach up to 25 μg m^{-3}, typically contributing 15–25% of total $PM_{2.5}$ mass[5,38,39]. Nitrate concentrations are much higher in winter than in summer, because low temperatures favour the particulate phase of nitrate. The model tends to be too high in summer 2013, but concentrations are then generally low. There is no systematic model bias in winter when concentrations are high.

Figure 2 shows the daily 2014–2019 time series of observed wintertime total $PM_{2.5}$ and its nitrate component in Beijing, as well as the mass ratio of nitrate to total $PM_{2.5}$, averaged for each winter.

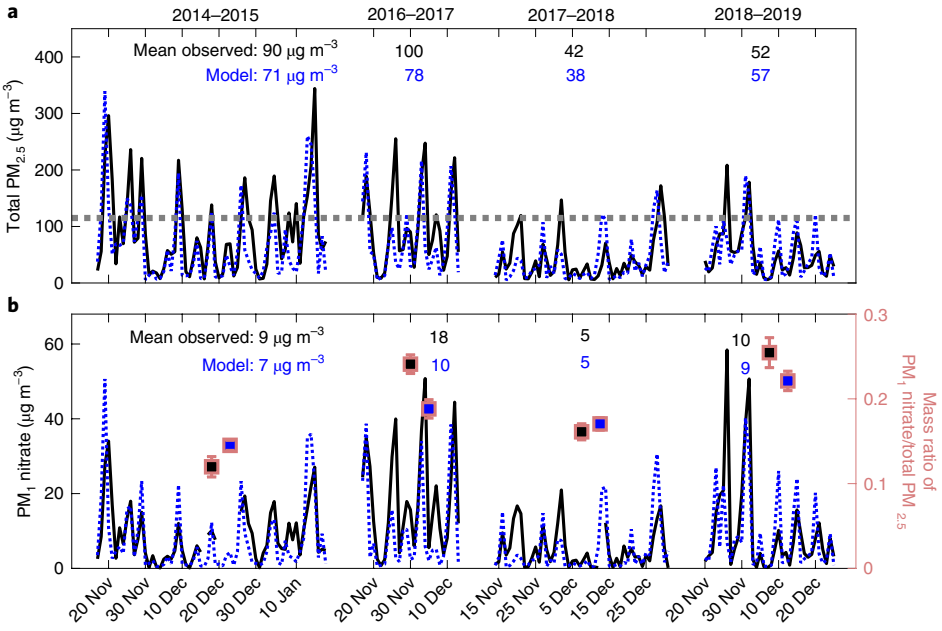

Fig. 2 | $PM_{2.5}$ and nitrate trends in Beijing. a,**b**, Time series of daily total $PM_{2.5}$ (**a**) and PM_1 nitrate (**b**) in Beijing for winters in 2014–2019. Also shown in **b** is the mass ratio of PM_1 nitrate to total $PM_{2.5}$ averaged for each winter (filled rectangles) at 35% relative humidity (RH)[49], with error bars representing the standard error of the mean among days for each winter. $PM_{2.5}$ concentrations (measured at 35% RH) are averages for the 12 MEE sites in Beijing. Nitrate observations were made at the Institute of Atmospheric Physics, Chinese Academy of Sciences, in downtown Beijing (116.37° E, 39.97° N) with a high-resolution time-of-flight aerosol mass spectrometer (HR-ToF-AMS; Aerodyne Research) for the winters of 2014–2015, 2016–2017 and 2018–2019 and an aerosol chemical speciation monitor (ACSM; Aerodyne Research) for winter 2017–2018[12,13]. Nitrate is measured as PM_1 (particles with diameter less than 1 μm), and we assume that this accounts for the bulk of $PM_{2.5}$ nitrate. The dashed line in **a** indicates the 115 μg m^{-3} threshold that separates lightly polluted and moderately polluted days in the Chinese Ambient Air Quality Index Classification Scheme, and is used here to diagnose winter haze conditions. Inset numbers are total $PM_{2.5}$ and PM_1 nitrate concentrations averaged over the observation period in each winter.

Winter mean $PM_{2.5}$ decreased over the five-year period, and winter haze events (daily $PM_{2.5} > 115\,\mu g\,m^{-3}$) decreased greatly in frequency. However, the winter mean nitrate did not decrease and actually increased on haze days, with 24-h values in 2018–2019 as high as 58 μg m^{-3}. The nitrate contribution to total $PM_{2.5}$ doubled from 12% in winter 2014–2015 to 25% in winter 2018–2019. Persistently high $PM_{2.5}$ nitrate is also observed at Handan, another site in the North China Plain (Supplementary Fig. 1). Winter 2017–2018 had low values for all $PM_{2.5}$ components, reflecting favourable meteorology as well as particularly aggressive restrictions on coal use that winter[3,10]. Also shown in Fig. 2 are the corresponding GEOS-Chem model results. The model generally reproduces the day-to-day variations of total $PM_{2.5}$ and its nitrate component, including the nitrate peaks on haze days and the increasing nitrate fraction from 2013–2014 to 2018–2019.

Trends of other major $PM_{2.5}$ components and for other sites across China between 2013 and 2018 are shown in Supplementary Fig. 2. All sites show a similarly small trend in nitrate, resulting in an increasing relative contribution of nitrate to total $PM_{2.5}$ mass. Nitrate in summer shows a much steeper decrease than in winter (Extended Data Fig. 4 and Supplementary Fig. 3)[5,40]. Superimposed on the long-term trends is large month-to-month variability driven by meteorology, which the model also captures.

Meteorological drivers of nitrate trends

$PM_{2.5}$ nitrate is highly sensitive to meteorological variables, not only transport and precipitation, but also temperature and relative humidity (RH), affecting ammonium nitrate formation thermodynamics[41]. Figure 3a,b show the 2013–2017 nitrate trends over the North China Plain simulated by GEOS-Chem, with and without impacts from interannual variations in meteorology. Annual mean nitrate decreases by 17% in the standard simulation, largely following the trend in winter when nitrate is highest. Remarkably, we find that this decrease is due to meteorological rather than to emission trends, because annual mean nitrate in the fixed-meteorology simulation shows no decrease, and nitrate in winter slightly increases, despite the 22% decrease of NO_x emissions. Consistent with this result, model interpretation of the observed decreases of annual mean nitrate at North China Plain sites shows that they are driven by meteorology rather than a decrease in NO_x emissions (Supplementary Fig. 4). The temperature increased and RH decreased from 2013 to 2017 over the North China Plain on an annual mean basis, and particularly in winter (Extended Data Fig. 5), and this would drive a decrease in nitrate. $PM_{2.5}$ nitrate increased by 30–40% from 2013 to 2017 under winter haze conditions in both the standard and fixed-meteorology simulations.

Chemical drivers of nitrate trends

To diagnose the chemical drivers of the particulate nitrate trends in the model, we write a simple mass balance representation for the mean particulate nitrate concentration $[NO_3^-]$ in the boundary layer:

$$[NO_3^-] = P(NO_3^T)\left(\frac{1}{\frac{1}{\tau_{NO_3^T,dep}} + \frac{1}{\tau_{vent}}}\right)\frac{[NO_3^-]}{[NO_3^T]} \quad (1)$$

where $P(NO_3^T)$ is the rate of NO_3^T production in the boundary layer, $\tau_{NO_3^T,dep}$ is the lifetime of NO_3^T against deposition, and τ_{vent} is the timescale for ventilation, which we can estimate as a few days. $P(NO_3^T)$ is in turn given by

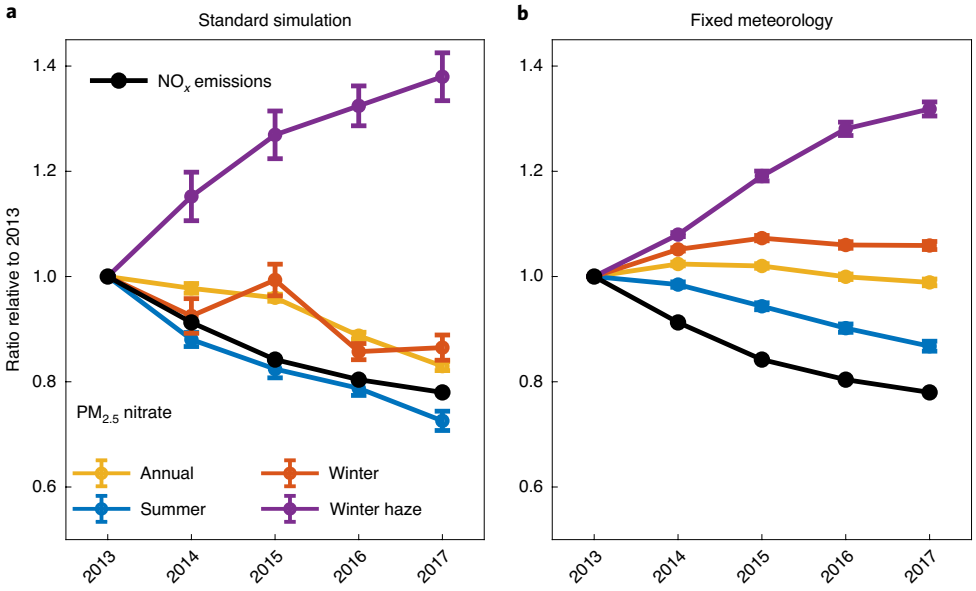

Fig. 3 | 2013–2017 trends of $PM_{2.5}$ nitrate concentrations in the North China Plain relative to 2013 values. The results are from the GEOS-Chem model driven by 2013–2017 MEIC emissions. **a**, Standard simulation with year-by-year changes in meteorology. **b**, Results with 2017 meteorology applied to all years. Model values are sampled at the 63 MEE observation sites in the North China Plain and then averaged. Vertical bars are the standard error of the mean $PM_{2.5}$ nitrate for the 63 MEE sites. Winter haze days are defined in the same way as in Fig. 2. The increasing trend of $PM_{2.5}$ nitrate under winter haze conditions holds as the threshold increases from 115 μg m^{-3} to 150 μg m^{-3} (the threshold that separates moderately polluted and heavily polluted days). Here, we chose 115 μg m^{-3} to ensure a sufficient sample size. NO_x emission trends from the MEIC inventory are also shown.

$$P\left(NO_3{}^T\right) = \frac{E_{NO_x}}{h}\frac{1}{1+\frac{\tau_{NO_x,chem}}{\tau_{vent}}} \quad (2)$$

where E_{NO_x} is the NO_x emission flux, h is the boundary layer depth and $\tau_{NO_x,chem}$ is the chemical lifetime of NO_x against oxidation to $NO_3{}^T$. $\tau_{NO_3{}^T,dep}$ can be expressed as[42]

$$\tau_{NO_3{}^T,dep} = \frac{h\left[NO_3{}^T\right]}{F_{NO_3{}^T}} = \frac{h}{v_p\left(k+(1-k)\frac{\left[NO_3{}^-\right]}{\left[NO_3{}^T\right]}\right)} \quad (3)$$

where $F_{NO_3{}^T} = F_{NO_3{}^-} + F_{HNO_3}$ is the total (wet and dry) deposition flux of $NO_3{}^T$, $v_p = F_{NO_3{}^-}/\left[NO_3{}^-\right]$ is the total (wet and dry) deposition velocity for particulate nitrate in the boundary layer (neglecting scavenging above the boundary layer), and k is the ratio of the HNO_3 and particulate nitrate deposition velocities. k ranges from about 5 to 15 for wet and dry deposition[34,42,43], so $\tau_{NO_3{}^T,dep}$ is highly sensitive to changes in the $[NO_3{}^-]/[NO_3{}^T]$ ratio when this ratio exceeds 0.9. Accordingly, the sensitivity of $[NO_3{}^-]$ in equation (1) to a change in the $[NO_3{}^-]/[NO_3{}^T]$ ratio is greatly amplified by the sensitivity of $\tau_{NO_3{}^T,dep}$ in equation (3) to this ratio, a theoretical result previously derived in ref. [42]. Although highly simplified, this provides a diagnostic framework for understanding how 2013–2017 trends in nitrate reflect trends in the driving variables, assuming no trend in meteorology (fixed h and τ_{vent}).

Figure 4a shows the 2013–2017 model trends of the particulate fraction of total nitrate ($[NO_3{}^-]/[NO_3{}^T]$ molar ratio) in the North China Plain for summer mean, winter mean and winter haze conditions. The fraction increases with time because of the decreasing SO_2 and NO_x emissions as NH_3 emissions stay constant, but the change is no more than 10%. The $[NO_3{}^-]/[NO_3{}^T]$ ratio in winter exceeds 0.9, consistent with observations[13,21,22], because of high NH_3 concentrations and low temperatures. The thermodynamic regime of the sulfate–nitrate–ammonium (SNA) system can be diagnosed by the molar ratio $R = [NH_3{}^T]/(2\times[SO_4{}^{2-}] + [NO_3{}^T])$, where $NH_3{}^T$ denotes the sum of gas-phase ammonia and particulate ammonium ($NH_3{}^T \equiv NH_3 + NH_4{}^+$). $R > 1$ indicates ammonia in excess, while $R < 1$ indicates nitrate in excess[44]. We plot in Extended Data Fig. 6 the model values of R as a function of total SNA concentrations for 2013–2017 winter conditions. The values closely reproduce the observed R values and their relationship with SNA concentrations[44], showing consistent excess NH_3 ($R > 1$), and approaching a transition regime ($R \approx 1$) under winter haze conditions when sulfate and nitrate concentrations are high. In summer, high temperatures support higher partial pressures of both HNO_3 and NH_3, and ~40% of $NO_3{}^T$ remains in the gas phase.

Figure 4b shows the 2013–2017 model trends of NO_x chemical lifetime against conversion to $NO_3{}^T$ ($\tau_{NO_x,chem}$) and Fig. 4c shows the trends of $NO_3{}^T$ production ($P(NO_3{}^T)$), which reflect both the 22% decrease in NO_x emissions and the change in NO_x lifetime. From 2013 to 2017, the NO_x chemical lifetime remained nearly unchanged in summer, but decreased by 17% in winter on average and by 22% for winter haze days, consistent with the NO_2 trends observed from satellite and their simulation with GEOS-Chem[25]. Accordingly, $NO_3{}^T$ production decreased by 22% in summer (same as NO_x emissions), but only by 13% in winter and with no notable trend on winter haze days. The NO_x chemical lifetime in winter is 2–3 days, sufficiently long that changes in this lifetime would affect nitrate formation in the North China Plain through competition with ventilation. The decrease in NO_x lifetime over the 2013–2017 period could thus partly explain the lack of response of wintertime nitrate to NO_x emission controls, but it is insufficient to explain the increase of nitrate during winter haze conditions.

Figure 4d shows the 2013–2017 trends of $NO_3{}^T$ lifetime against removal by deposition $\left(\tau_{NO_3{}^T,dep}\right)$. The $NO_3{}^T$ lifetime increased by 27% in winter (on average) and by 37% on winter haze days, but by only 5% in summer. Because HNO_3 deposits about 5–15 times faster than particulate nitrate[34,42,43], one would expect deposition of $NO_3{}^T$

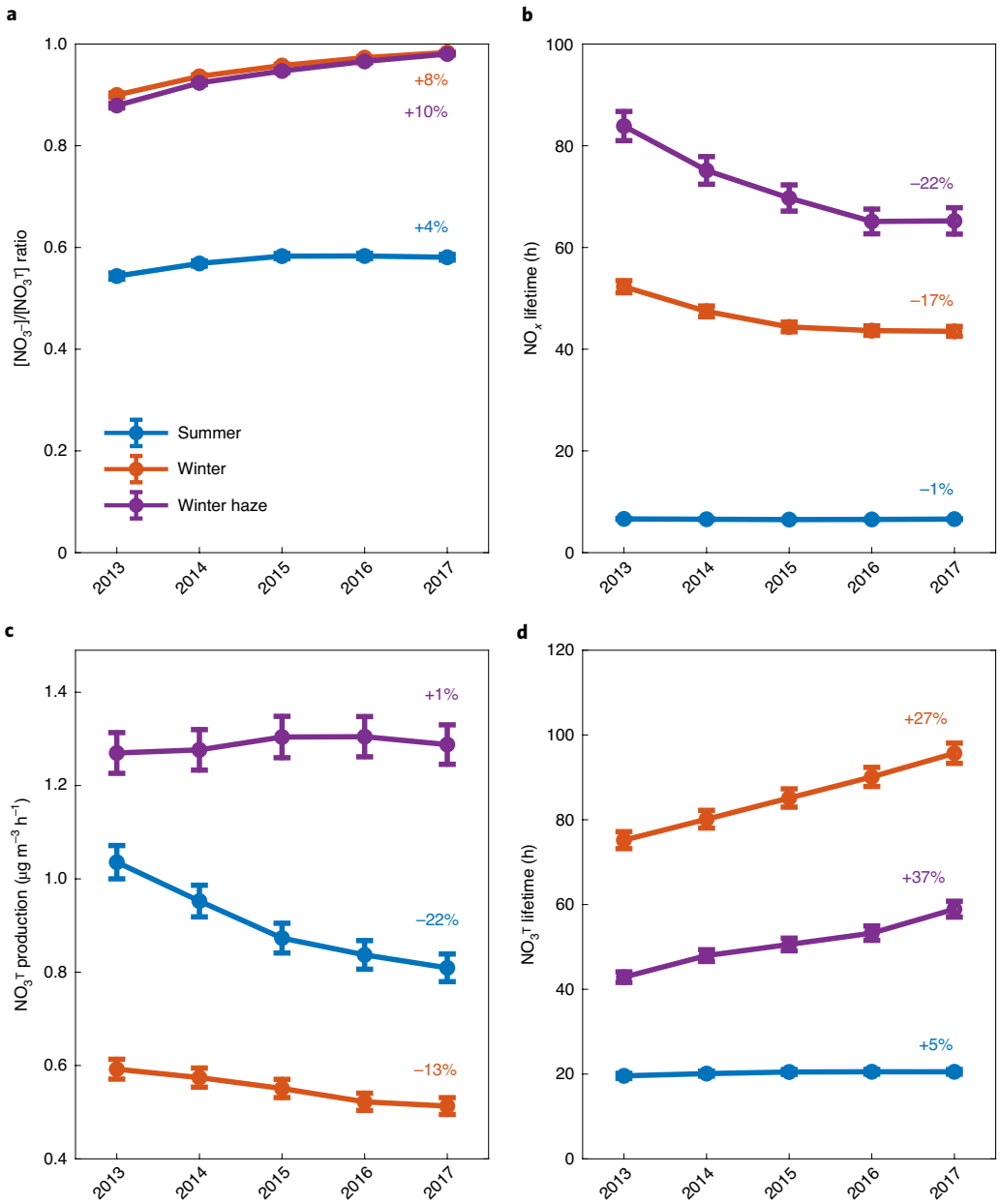

Fig. 4 | Factors contributing to the 2013–2017 trends of $PM_{2.5}$ nitrate over the North China Plain. a, Particulate fraction of total nitrate ($[NO_3^-]/[NO_3^T]$ molar ratio). **b**, NO_x lifetime against conversion to NO_3^T. **c**, NO_3^T production rate. **d**, NO_3^T lifetime against deposition. Values are from the GEOS-Chem model simulation with repeating 2017 meteorology and are shown for summer, winter and winter haze conditions. Winter haze days are defined in the same way as in Fig. 2. Production rates and lifetimes are averages for the boundary layer with heights of 2,000 m in summer, 1,500 m in winter and 320 m for winter haze conditions. For the NO_x lifetime calculation, we define NO_x as $NO + NO_2 + NO_3 + 2N_2O_5 + HONO + HNO_4 + ClNO_2$. Error bars are the standard error of the mean over the North China Plain region. Inset numbers are percent changes from 2013 to 2017.

to be dominated by HNO_3, and that is indeed the case in summer. In winter, however, the $[NO_3^-]/[NO_3^T]$ ratio is sufficiently large that particulate nitrate is an important contributor to NO_3^T deposition, and a small increase in $[NO_3^-]/[NO_3^T]$ (Fig. 4a) can drive a large increase in NO_3^T lifetime, thus amplifying its impact on particulate nitrate (equation (3)). We thus find in our simulation that particulate nitrate is responsible for 40% of wintertime NO_3^T deposition in 2013 but 60% in 2017, and that this effect of the $[NO_3^-]/[NO_3^T]$ ratio on NO_3^T deposition is the dominant factor explaining the increase of nitrate in winter haze. Our results for 2013–2017 relative trends in $PM_{2.5}$ nitrate, $[NO_3^-]/[NO_3^T]$ ratio and $[NO_3^T]$ lifetime are insensitive to the choice of wet deposition scheme (Extended Data Fig. 7).

An emission control strategy to decrease $PM_{2.5}$ nitrate

Decreasing the nitrate component of $PM_{2.5}$ is an increasing priority for improving $PM_{2.5}$ air quality in China. An emission control strategy must focus on the wintertime, when both $PM_{2.5}$ and the nitrate contribution are highest. A recent model study[9] found that reduction of both VOC and NO_x emissions by 30% decreased $PM_{2.5}$ nitrate by only 8.6% over the North China Plain in winter. Another avenue suggested by our analysis is to control NH_3 emissions to increase the small fraction of NO_3^T present as HNO_3 and hence drive faster NO_3^T deposition[42].

Figure 5 shows the simulated responses of $PM_{2.5}$ nitrate in the North China Plain to 10–50% reductions of SO_2, NO_x, VOCs, NH_3

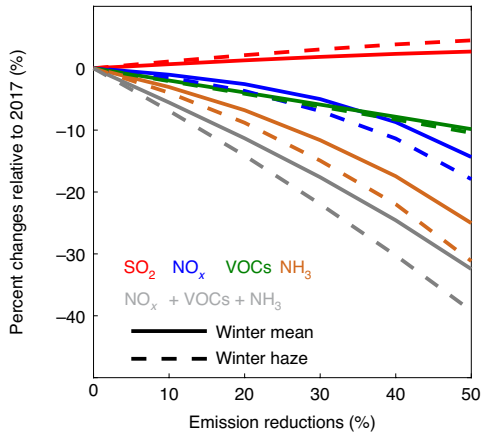

Fig. 5 | Percent changes of wintertime $PM_{2.5}$ nitrate in response to emission reductions in the North China Plain relative to 2017. Results are from GEOS-Chem simulations for the 2017 meteorological year including 10–50% individual emission reductions of SO_2, NO_x, VOCs, NH_3 and combined emission reductions of NO_x + VOCs + NH_3. Haze days are defined in the same way as in Fig. 2. The percent changes are for the mean wintertime or mean winter haze surface concentrations of $PM_{2.5}$ nitrate averaged over the North China Plain.

and (NO_x + VOCs + NH_3) emissions for average winter conditions and for winter haze days, relative to 2017 values. We find that NH_3 is the most effective lever for $PM_{2.5}$ nitrate control, particularly on winter haze days, consistent with the effect on NO_3^T lifetime. Reducing NH_3 emissions by any increment is beneficial. Reducing NH_3 emissions by 50% decreases $PM_{2.5}$ nitrate by 25% on average and by 31% on haze days. At that point, some winter days transit to NH_3-limited conditions (Supplementary Fig. 5), but we find that faster NO_3^T deposition from decreasing $[NO_3^-]/[NO_3^T]$ still accounts for 70% of the $PM_{2.5}$ nitrate decrease.

Reducing NO_x emissions is far less effective because it drives a decrease in NO_x lifetime, which offsets the decrease in NO_3^T production (equation (2)). Reducing NO_x emissions by up to 20% has no net effect on $PM_{2.5}$ nitrate, and even a 50% reduction has only a 14% benefit. Reducing VOC emissions (slowing down oxidant production) has only a weak effect: a 50% reduction decreases $PM_{2.5}$ nitrate by only 10%, because HONO photolysis (rather than formaldehyde or ozone photolysis) is the dominant wintertime source of oxidants in the model, consistent with observations[45]. Reducing both VOC and NO_x emissions by 30% decreases $PM_{2.5}$ nitrate by only 10%, consistent with ref. [9]. Combining NO_x, VOCs and NH_3 emission reductions provides limited benefit beyond NH_3 reduction alone, because NH_3 reduction causes NH_3 to become more limiting, which counters the benefit of NO_x and VOCs reductions. Continued reduction of SO_2 emissions increases nitrate by only a few percent because these emissions are already low and the $[NO_3^-]/[NO_3^T]$ ratio is already near unity. In terms of total $PM_{2.5}$, reducing NH_3 emissions by 50% decreases total $PM_{2.5}$ by 13% in winter, 18% during winter haze days and 14% for the annual mean (Extended Data Fig. 8).

Previous model studies found that NH_3 emission reductions led to particulate nitrate decrease, but attributed it simply to a shift of NO_3^T from the particle to the gas phase[24,37,46]. This was inconsistent with field observations showing consistently high $[NO_3^-]/[NO_3^T]$ ratios[13,21]. Our work solves this conundrum by pointing to changes in the NO_3^T lifetime against deposition driven by small changes in the $[NO_3^-]/[NO_3^T]$ ratio as the principal driver of the sensitivity of nitrate to NH_3 emissions in winter. The dominant source of NH_3 is from agriculture and could be controlled by limiting fertilizer application and better managing manure[37]. Fossil fuel combustion could be a major contributor to NH_3 emissions in Beijing[17,18,20], and this would provide another avenue for emission control.

In summary, we have explained the weak response of $PM_{2.5}$ nitrate to emission controls in China over the 2013–2017 period, and the increase of nitrate during winter haze pollution events in the North China Plain, through successful simulation with the GEOS-Chem model. We find that the dominant factor driving the observed nitrate trends is the increase in the lifetime of total nitrate (gas + particulate) against deposition as the particulate fraction of total nitrate approaches unity. From model sensitivity studies, we find that NH_3 emission reduction is most effective at decreasing $PM_{2.5}$ nitrate in winter, and that NO_x or VOC emission reductions are far less effective. There are a few sources of uncertainty in the model, for example in the assumption of bulk SNA thermodynamics[47] and in the land-use information driving dry deposition[35], but they do not manifest themselves as systematic biases. Our results point to the need to better understand the sources of NH_3 in urban China in winter as targets for emission controls.

Online content

Any methods, additional references, Nature Research reporting summaries, source data, extended data, supplementary information, acknowledgements, peer review information; details of author contributions and competing interests; and statements of data and code availability are available at https://doi.org/10.1038/s41561-021-00726-z.

Received: 25 June 2020; Accepted: 7 March 2021;
Published online: 26 April 2021

References

1. *Action Plan on Prevention and Control of Air Pollution* (in Chinese) (Chinese State Council, 2013); http://www.gov.cn/zwgk/2013-09/12/content_2486773.htm
2. Zhai, S. et al. Fine particulate matter ($PM_{2.5}$) trends in China, 2013–2018: separating contributions from anthropogenic emissions and meteorology. *Atmos. Chem. Phys.* **19**, 11031–11041 (2019).
3. Zhang, Q. et al. Drivers of improved $PM_{2.5}$ air quality in China from 2013 to 2017. *Proc. Natl Acad. Sci. USA* **116**, 24463–24469 (2019).
4. Liu, M. et al. Rapid SO_2 emission reductions significantly increase tropospheric ammonia concentrations over the North China Plain. *Atmos. Chem. Phys.* **18**, 17933–17943 (2018).
5. Zhou, W. et al. Response of aerosol chemistry to clean air action in Beijing, China: insights from two-year ACSM measurements and model simulations. *Environ. Pollut.* **255**, 113345 (2019).
6. Zheng, B. et al. Trends in China's anthropogenic emissions since 2010 as the consequence of clean air actions. *Atmos. Chem. Phys.* **18**, 14095–14111 (2018).
7. Gao, M. et al. China's emission control strategies have suppressed unfavorable influences of climate on wintertime $PM_{2.5}$ concentrations in Beijing since 2002. *Atmos. Chem. Phys.* **20**, 1497–1505 (2020).
8. *Regional Air Quality Has Improved Significantly, but Prevention and Control of Air Pollution Still Has a Long Way to Go* (in Chinese) (National Center for Atmospheric Pollution Control, 2020); https://mp.weixin.qq.com/s/5KoDFQrqtmJ4OXiL3LWlug
9. Fu, X. et al. Persistent heavy winter nitrate pollution driven by increased photochemical oxidants in northern China. *Environ. Sci. Technol.* **54**, 3881–3889 (2020).
10. Cheng, J. et al. Dominant role of emission reduction in $PM_{2.5}$ air quality improvement in Beijing during 2013–2017: a model-based decomposition analysis. *Atmos. Chem. Phys.* **19**, 6125–6146 (2019).
11. Shao, P. et al. Characterizing remarkable changes of severe haze events and chemical compositions in multi-size airborne particles (PM_1, $PM_{2.5}$ and PM_{10}) from January 2013 to 2016–2017 winter in Beijing, China. *Atmos. Environ.* **189**, 133–144 (2018).
12. Xu, W. et al. Changes in aerosol chemistry from 2014 to 2016 in winter in Beijing: insights from high-resolution aerosol mass spectrometry. *J. Geophys. Res. Atmos.* **124**, 1132–1147 (2019).
13. Song, S. et al. Thermodynamic modeling suggests declines in water uptake and acidity of inorganic aerosols in Beijing winter haze events during 2014/2015–2018/2019. *Environ. Sci. Technol. Lett.* **6**, 3881–3889 (2019).
14. Li, H. et al. Rapid transition in winter aerosol composition in Beijing from 2014 to 2017: response to clean air actions. *Atmos. Chem. Phys.* **19**, 11485–11499 (2019).

15. Lu, K. et al. Fast photochemistry in wintertime haze: consequences for pollution mitigation strategies. *Environ. Sci. Technol.* **53**, 10676–10684 (2019).
16. Xu, Q. et al. Nitrate dominates the chemical composition of $PM_{2.5}$ during haze event in Beijing, China. *Sci. Total Environ.* **689**, 1293–1303 (2019).
17. Pan, Y. et al. Fossil fuel combustion-related emissions dominate atmospheric ammonia sources during severe haze episodes: evidence from ^{15}N-stable isotope in size-resolved aerosol ammonium. *Environ. Sci. Technol.* **50**, 8049–8056 (2016).
18. Sun, K. et al. Vehicle emissions as an important urban ammonia source in the United States and China. *Environ. Sci. Technol.* **51**, 2472–2481 (2017).
19. Chang, Y. et al. The importance of vehicle emissions as a source of atmospheric ammonia in the megacity of Shanghai. *Atmos. Chem. Phys.* **16**, 3577–3594 (2016).
20. Bhattarai, N. et al. Sources of gaseous NH_3 in urban Beijing from parallel sampling of NH_3 and NH_4^+, their nitrogen isotope measurement and modeling. *Sci. Total Environ.* **747**, 141361 (2020).
21. Guo, H. et al. Effectiveness of ammonia reduction on control of fine particle nitrate. *Atmos. Chem. Phys.* **18**, 12241–12256 (2018).
22. Wang, G. et al. Persistent sulfate formation from London fog to Chinese haze. *Proc. Natl Acad. Sci. USA* **113**, 13630–13635 (2016).
23. Lachatre, M. et al. The unintended consequence of SO_2 and NO_2 regulations over China: increase of ammonia levels and impact on $PM_{2.5}$ concentrations. *Atmos. Chem. Phys.* **19**, 6701–6716 (2019).
24. Fu, X. et al. Increasing ammonia concentrations reduce the effectiveness of particle pollution control achieved via SO_2 and NO_x emissions reduction in East China. *Environ. Sci. Technol. Lett.* **4**, 221–227 (2017).
25. Shah, V. et al. Effect of changing NO_x lifetime on the seasonality and long-term trends of satellite-observed tropospheric NO_2 columns over China. *Atmos. Chem. Phys.* **20**, 1483–1495 (2020).
26. Jaeglé, L. et al. Nitrogen oxides emissions, chemistry, deposition and export over the Northeast United States during the WINTER Aircraft Campaign. *J. Geophys. Res. Atmos.* **123**, 12368–12393 (2018).
27. Wang, H. et al. Fast particulate nitrate formation via N_2O_5 uptake aloft in winter in Beijing. *Atmos. Chem. Phys.* **18**, 10483–10495 (2018).
28. Wang, H. et al. High N_2O_5 concentrations observed in urban Beijing: implications of a large nitrate formation pathway. *Environ. Sci. Technol. Lett.* **4**, 416–420 (2017).
29. Leung, D. M. et al. Wintertime particulate matter decrease buffered by unfavorable chemical processes despite emissions reductions in China. *Geophys. Res. Lett.* **47**, e2020GL087721 (2020).
30. Womack, C. C. et al. An odd oxygen framework for wintertime ammonium nitrate aerosol pollution in urban areas: NO_x and VOC control as mitigation strategies. *Geophys. Res. Lett.* **46**, 4971–4979 (2019).
31. Geng, G. et al. Chemical composition of ambient $PM_{2.5}$ over China and relationship to precursor emissions during 2005–2012. *Atmos. Chem. Phys.* **17**, 1–25 (2017).
32. Li, K. et al. A two-pollutant strategy for improving ozone and particulate air quality in China. *Nat. Geosci.* **12**, 906–910 (2019).
33. Lu, X. et al. Exploring 2016–2017 surface ozone pollution over China: source contributions and meteorological influences. *Atmos. Chem. Phys.* **19**, 8339–8361 (2019).
34. Luo, G., Yu, F. & Schwab, J. Revised treatment of wet scavenging processes dramatically improves GEOS-Chem 12.0.0 simulations of nitric acid, nitrate and ammonium over the United States. *Geosci. Model Dev.* **12**, 3439–3447 (2019).
35. Xu, W., Zhang, L. & Liu, X. A database of atmospheric nitrogen concentration and deposition from the nationwide monitoring network in China. *Sci. Data* **6**, 51 (2019).
36. Liu, Z. et al. Characteristics of $PM_{2.5}$ mass concentrations and chemical species in urban and background areas of China: emerging results from the CARE-China network. *Atmos. Chem. Phys.* **18**, 8849–8871 (2018).
37. Liu, M. et al. Ammonia emission control in China would mitigate haze pollution and nitrogen deposition, but worsen acid rain. *Proc. Natl Acad. Sci. USA* **116**, 7760–7765 (2019).
38. Xie, Y. et al. Characteristics of chemical composition and seasonal variations of $PM_{2.5}$ in Shijiazhuang, China: impact of primary emissions and secondary formation. *Sci. Total Environ.* **677**, 215–229 (2019).
39. Duan, J. et al. Summertime and wintertime atmospheric processes of secondary aerosol in Beijing. *Atmos. Chem. Phys.* **20**, 3793–3807 (2020).
40. Li, H. et al. Nitrate-driven urban haze pollution during summertime over the North China Plain. *Atmos. Chem. Phys.* **18**, 5293–5306 (2018).
41. Seinfeld, J. H & Pandis, S. N. *Atmospheric Chemistry and Physics* (Wiley, 2016).
42. Nenes, A. et al. Aerosol acidity and liquid water content regulate the dry deposition of inorganic reactive nitrogen. *Atmos. Chem. Phys. Discuss.* **2020**, 1–25 (2020).
43. Zhang, L. et al. Nitrogen deposition to the United States: distribution, sources and processes. *Atmos. Chem. Phys.* **12**, 4539–4554 (2012).
44. Xu, Z. et al. High efficiency of livestock ammonia emission controls in alleviating particulate nitrate during a severe winter haze episode in northern China. *Atmos. Chem. Phys.* **19**, 5605–5613 (2019).
45. Tan, Z. et al. Wintertime photochemistry in Beijing: observations of RO_x radical concentrations in the North China Plain during the BEST-ONE campaign. *Atmos. Chem. Phys.* **18**, 12391–12411 (2018).
46. Geng, G. et al. Impact of China's air pollution prevention and control action plan on $PM_{2.5}$ chemical composition over eastern China. *Sci. China Earth Sci.* **62**, 1872–1884 (2019).
47. Wexler, A. S. & Seinfeld, J. H. Analysis of aerosol ammonium nitrate: departures from equilibrium during SCAQS. *Atmos. Environ. A* **26**, 579–591 (1992).
48. Xin, J. et al. The campaign on atmospheric aerosol research network of china: CARE-China. *Bull. Am. Meteorol.* **96**, 1137–1155 (2014).
49. Kim, P. S. et al. Sources, seasonality, and trends of southeast US aerosol: an integrated analysis of surface, aircraft, and satellite observations with the GEOS-Chem chemical transport model. *Atmos. Chem. Phys.* **15**, 10411–10433 (2015).

Methods

GEOS-Chem simulations. We used the GEOS-Chem model version 12.3.1 in a nested-grid simulation over East Asia (60°–150° E, 10° S–55° N) with a horizontal resolution of 0.5° × 0.625°. The GEOS-Chem model simulates detailed ozone–NO_x–VOC–aerosol–halogen chemistry[49–52] and is driven by meteorological data from NASA Modern-Era Retrospective Analysis for Research and Applications, Version 2 (MERRA-2). A number of previous studies have applied GEOS-Chem to simulations of $PM_{2.5}$, NO_2 and ozone air quality in China, showing consistency between observations and model results[25,31–33,53].

Monthly anthropogenic emissions over China, including agricultural NH_3, are taken from MEIC for 2013–2017[6] and from the MIX inventory for 2010 over other Asian countries[54]. The simulation for winter 2018–2019 in Fig. 2 uses 2017 MEIC emissions with SO_2 emissions reduced by 26% and primary organic carbon (OC) and black carbon (BC) emissions reduced by 13%, based on the observed decreases of SO_2 and CO from 2017 to 2018 at the MEE sites. Fine anthropogenic dust emissions from combustion and industrial sources are derived from MEIC as the residual of anthropogenic primary emissions of $PM_{2.5}$, after excluding primary organic aerosol (POA; here we use a uniform POA-to-primary-organic-carbon mass ratio of 1.7)[55], BC and primary sulfate[56]. Natural emissions include NO_x from lightning[57] and soil[58]. Biomass burning emissions are taken from the Global Fire Emissions Database version 4 (GFED4)[59].

$PM_{2.5}$ is simulated in GEOS-Chem as the sum of sulfate, nitrate, ammonium, organic aerosol (OA ≡ primary OA + secondary OA), BC, fine dust and fine sea salt components. Sulfate production is described in ref. [60]. Nitrate production is described in ref. [25]. The thermodynamic equilibrium of SNA particles with the gas phase is computed with ISORROPIA II[50,61] assuming an aqueous aerosol. We use a simple secondary organic aerosol formation scheme following ref. [49]. Natural dust aerosols are simulated as described by ref. [62]. Sea salt aerosol is simulated as described in ref. [63].

Dry deposition of gases and particles follows a standard resistance-in-series scheme[64]. It includes a recent model update (from version 12.6.0) to improve the representation of HNO_3 dry deposition at low temperatures[26], but we found that this had a negligible influence on our results. Wet deposition of gases and particles includes in-cloud scavenging, below-cloud scavenging and scavenging in convective updrafts[65–68]. Here, we use an updated GEOS-Chem wet scavenging scheme for HNO_3 and particulate nitrate deposition[34], introduced in version 12.8.0, that features faster below-cloud scavenging of HNO_3 limited by molecular diffusion to raindrops.

Extended Data Fig. 1 and Supplementary Fig. 6 compare nitrate wet deposition fluxes in the model to observations from the National Nitrogen Deposition Monitoring Network (NNDMN)[35]. The model reproduces the observed spatial and seasonal variations. The NNDMN also reports dry deposition fluxes by applying GEOS-Chem deposition velocities to surface measurements of HNO_3 and NO_3^- concentrations, but the HNO_3 concentrations (which usually drive total dry deposition) cannot be usefully compared to GEOS-Chem model values because they are highly sensitive to local surface type, atmospheric stability and measurement altitude[43].

A number of GEOS-Chem simulations were carried out in this study: (1) a 'standard simulation' with emissions and meteorology changing year by year from 2013 to 2017; (2) a 'fixed-meteorology simulation' with emissions changing from 2013 to 2017 but with meteorology fixed at 2017; (3) 'future emission control simulations' with individual 10–50% emission reductions for SO_2, NO_x, VOCs, NH_3 and combined emission reductions for NO_x + VOCs + NH_3 applied uniformly over China relative to the baseline simulation for 2017. The latter simulations (Fig. 5) were done at a horizontal resolution of 4° × 5°, but we found that this had no notable impact on the results.

Data availability

Surface $PM_{2.5}$ observations across China from the China Ministry of Ecology and Environment (MEE) national network can be downloaded from quotsoft.net/air. The anthropogenic emission inventory is from www.meicmodel.org. MERRA-2 reanalysis data are from https://gmao.gsfc.nasa.gov/reanalysis/MERRA-2/data_access/. Information about the observed $PM_{2.5}$ species concentrations used in this work are summarized in the Supplementary Table. $PM_{2.5}$ species observation data are deposited at https://doi.org/10.7910/DVN/VHFTLQ. The National Nitrogen Deposition Monitoring Network (NNDMN) version 1.0 database is from ref. [35]. Source data are provided with this paper.

Code availability

The GEOS-Chem model code version 12.3.1 is open source (https://doi.org/10.5281/zenodo.2633278). Code for calculations and data processing is available from the corresponding author upon request.

References

50. Pye, H. O. T. et al. Effect of changes in climate and emissions on future sulfate–nitrate–ammonium aerosol levels in the United States. *J. Geophys. Res. Atmos.* **114**, D01205 (2009).
51. Mao, J. et al. Ozone and organic nitrates over the eastern United States: sensitivity to isoprene chemistry. *J. Geophys. Res. Atmos.* **118**, 11256–11268 (2013).
52. Sherwen, T. et al. Global impacts of tropospheric halogens (Cl, Br, I) on oxidants and composition in GEOS-Chem. *Atmos. Chem. Phys.* **16**, 12239–12271 (2016).
53. Dang, R. & Liao, H. Severe winter haze days in the Beijing–Tianjin–Hebei region from 1985 to 2017 and the roles of anthropogenic emissions and meteorology. *Atmos. Chem. Phys.* **19**, 10801–10816 (2019).
54. Li, M. et al. MIX: a mosaic Asian anthropogenic emission inventory under the international collaboration framework of the MICS-Asia and HTAP. *Atmos. Chem. Phys.* **17**, 34813–34869 (2017).
55. Philip, S. et al. Spatially and seasonally resolved estimate of the ratio of organic mass to organic carbon. *Atmos. Environ.* **87**, 34–40 (2014).
56. Philip, S. et al. Anthropogenic fugitive, combustion and industrial dust is a significant, underrepresented fine particulate matter source in global atmospheric models. *Environ. Res. Lett.* **12**, 044018 (2017).
57. Murray, L. T., Jacob, D. J., Logan, J. A., Hudman, R. C. & Koshak, W. J. Optimized regional and interannual variability of lightning in a global chemical transport model constrained by LIS/OTD satellite data. *J. Geophys. Res. Atmos.* **117**, D20307 (2012).
58. Hudman, R. C. et al. Steps towards a mechanistic model of global soil nitric oxide emissions: implementation and space based-constraints. *Atmos. Chem. Phys.* **12**, 7779–7795 (2012).
59. van der Werf, G. R. et al. Global fire emissions estimates during 1997–2016. *Earth Syst. Sci. Data* **9**, 697–720 (2017).
60. Shao, J. et al. Heterogeneous sulfate aerosol formation mechanisms during wintertime Chinese haze events: air quality model assessment using observations of sulfate oxygen isotopes in Beijing. *Atmos. Chem. Phys.* **19**, 6107–6123 (2019).
61. Fountoukis, C. & Nenes, A. ISORROPIA II: a computationally efficient thermodynamic equilibrium model for K^+–Ca^{2+}–Mg^{2+}–NH_4^+–Na^+–SO_4^{2-}–NO_3^-–Cl^-–H_2O aerosols. *Atmos. Chem. Phys.* **7**, 4639–4659 (2007).
62. Fairlie, T. D., Jacob, D. J. & Park, R. J. The impact of transpacific transport of mineral dust in the United States. *Atmos. Environ.* **41**, 1251–1266 (2007).
63. Jaegle, L., Quinn, P. K., Bates, T. S., Alexander, B. & Lin, J. T. Global distribution of sea salt aerosols: new constraints from in situ and remote sensing observations. *Atmos. Chem. Phys.* **11**, 3137–3157 (2011).
64. Wesely, M. L. Parameterization of surface resistances to gaseous dry deposition in regional-scale numerical models. *Atmos. Environ.* **23**, 1293–1304 (1989).
65. Liu, H., Jacob, D. J., Bey, I. & Yantosca, R. M. Constraints from ^{210}Pb and ^{7}Be on wet deposition and transport in a global three-dimensional chemical tracer model driven by assimilated meteorological fields. *J. Geophys. Res. Atmos.* **106**, 12109–12128 (2001).
66. Amos, H. M. et al. Gas-particle partitioning of atmospheric Hg(II) and its effect on global mercury deposition. *Atmos. Chem. Phys.* **12**, 591–603 (2012).
67. Wang, Q. et al. Sources of carbonaceous aerosols and deposited black carbon in the Arctic in winter–spring: implications for radiative forcing. *Atmos. Chem. Phys.* **11**, 12453–12473 (2011).
68. Wang, Q. et al. Global budget and radiative forcing of black carbon aerosol: constraints from pole-to-pole (HIPPO) observations across the Pacific. *J. Geophys. Res. Atmos.* **119**, 195–206 (2014).
69. Luo, G., Yu, F. & Moch, J. M. Further improvement of wet process treatments in GEOS-Chem v12.6.0: impact on global distributions of aerosols and aerosol precursors. *Geosci. Model Dev.* **13**, 2879–2903 (2020).
70. Ji, D. et al. Impact of air pollution control measures and regional transport on carbonaceous aerosols in fine particulate matter in urban Beijing, China: insights gained from long-term measurement. *Atmos. Chem. Phys.* **19**, 8569–8590 (2019).
71. Zhao, L. et al. Changes of chemical composition and source apportionment of $PM_{2.5}$ during 2013–2017 in urban Handan, China. *Atmos. Environ.* **206**, 119–131 (2019).
72. Chang, Y. et al. Assessment of carbonaceous aerosols in Shanghai, China—Part 1: long-term evolution, seasonal variations and meteorological effects. *Atmos. Chem. Phys.* **17**, 9945–9964 (2017).
73. Ding, A. et al. Significant reduction of $PM_{2.5}$ in eastern China due to regional-scale emission control: evidence from SORPES in 2011–2018. *Atmos. Chem. Phys.* **19**, 11791–11801 (2019).

Acknowledgements

This work was funded by the Harvard–NUIST Joint Laboratory for Air Quality and Climate, the Samsung $PM_{2.5}$ Strategic Research Program and Samsung Advanced Institute of Technology. H.L. is supported by the National Key Research and Development Program of China (grant no. 2019YFA0606804). G.L. and F.Y. acknowledge funding support from NASA under grant no. NNX17AG35G. Y.S. acknowledges support from the Beijing Municipal Natural Science Foundation (8202049).

Author contributions

S.Z., D.J.J. and H.L. designed research. S.Z. performed research. X.W., V.S., J.M.M., K.H.B., L.S., G.L. and F.Y. helped with model simulations. Z.L., T.W., Y.S., L.W., M.Q., J.T., K.G., H.X., T.Z. and Y.W. helped with data collection. X.W., V.S., K.L., S.S., Y.Z., H.C.L. and H.C. helped with results interpretation. Q.Z. provided the MEIC emission inventory. S.Z. and D.J.J. wrote the paper with input from all other authors.

Competing interests

The authors declare no competing interests.

Additional information

Extended data is available for this paper at https://doi.org/10.1038/s41561-021-00726-z.

Supplementary information The online version contains supplementary material available at https://doi.org/10.1038/s41561-021-00726-z.

Correspondence and requests for materials should be addressed to D.J.J.

Peer review information *Nature Geoscience* thanks the anonymous reviewers for their contribution to the peer review of this work. Primary Handling Editor: Rebecca Neely.

Reprints and permissions information is available at www.nature.com/reprints.

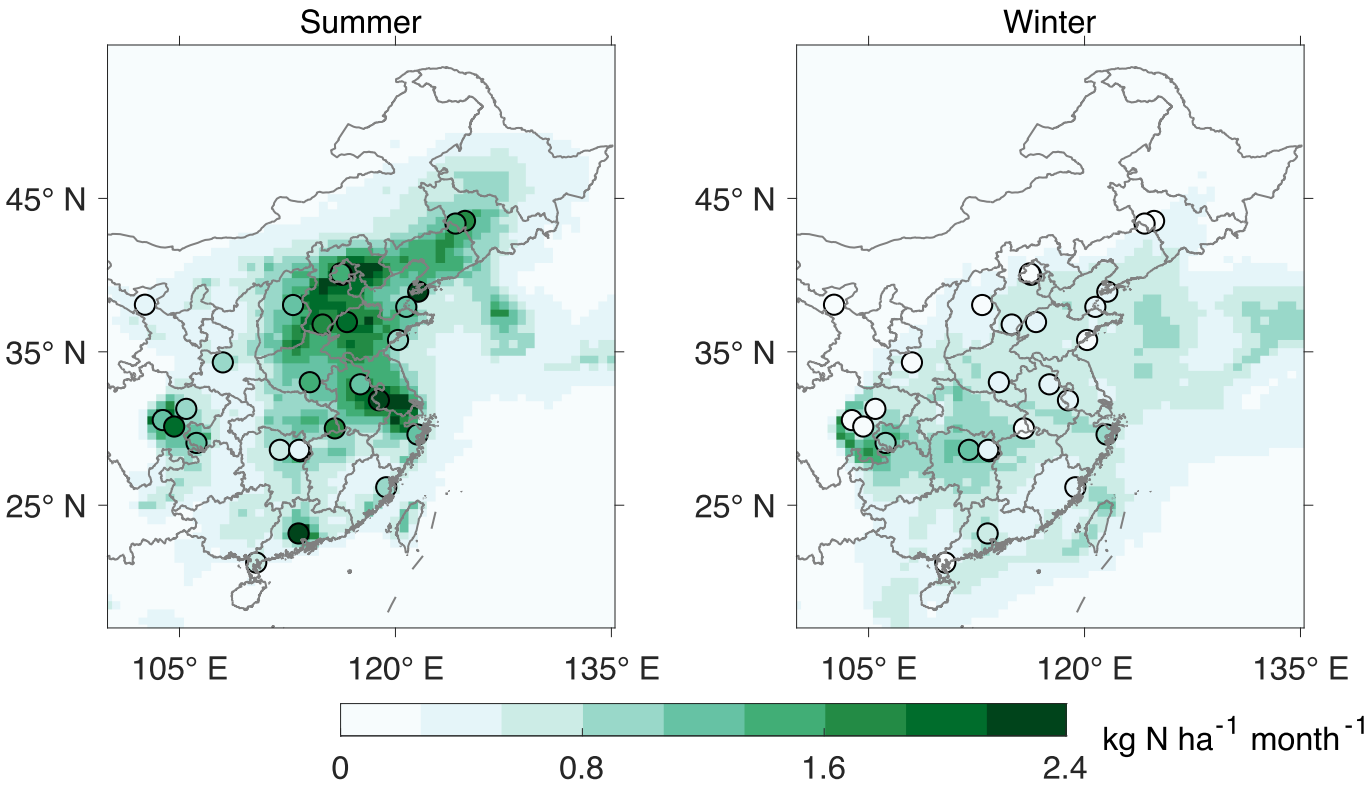

Extended Data Fig. 1 | Spatial distribution of measured (filled circles) and modeled (gridded background) 3-year (2013-2015) averaged summer mean and winter mean nitrate wet deposition fluxes. Measurements are from the National Nitrogen Deposition Monitoring Network (NNDMN) version 1.0 database[35]. Comprehensive global evaluation of the updated wet scavenging scheme can be found in refs. [34,69].

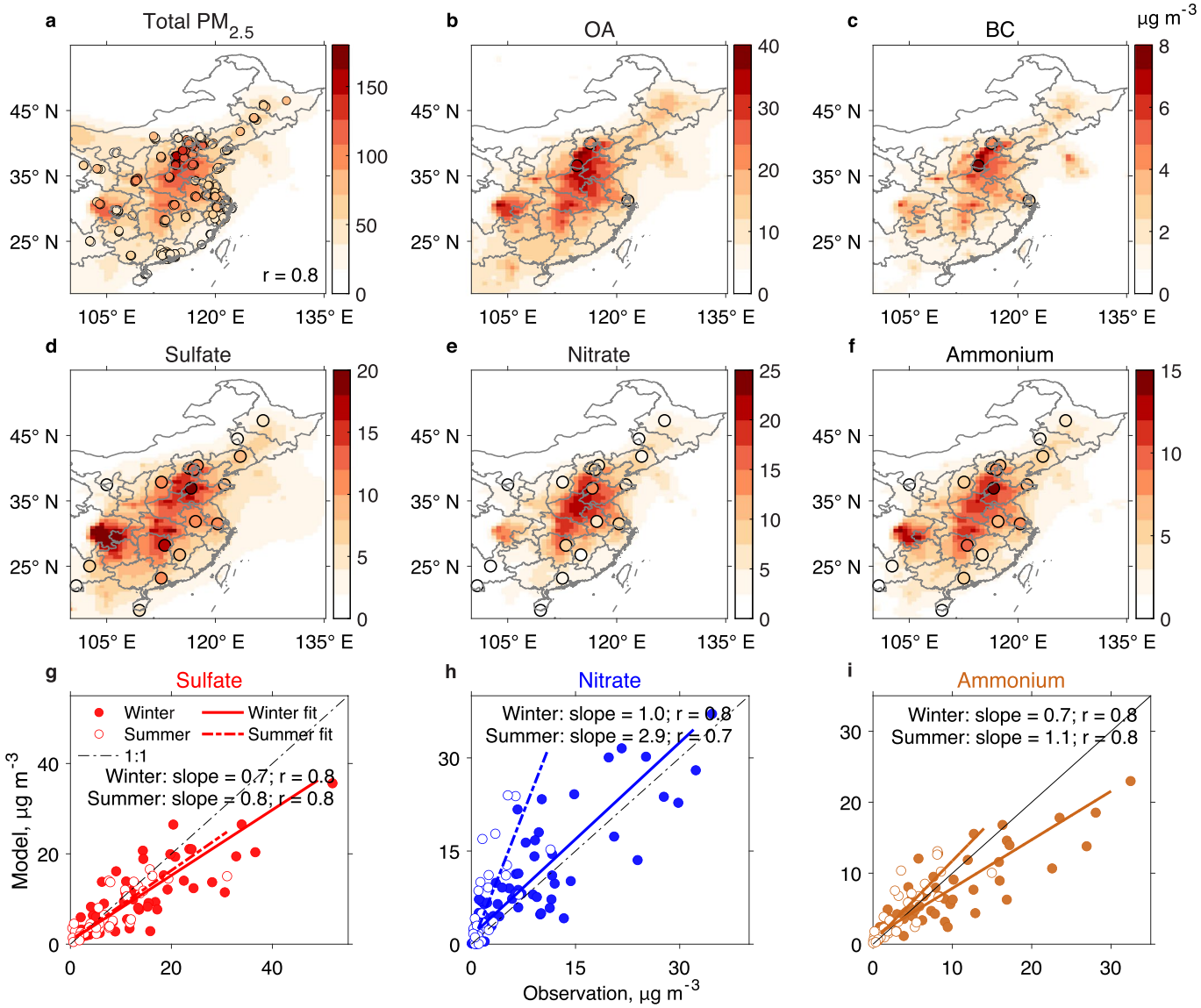

Extended Data Fig. 2 | Spatial and seasonal patterns of the mass concentrations of $PM_{2.5}$ and its major components (OA, BC, sulfate, nitrate, and ammonium) over China in 2013. a-f, Spatial distributions of observed annual mean concentrations (circles) are compared to the GEOS-Chem model (background). **g-i**, Scatter plots of observed and modeled monthly mean sulfate, nitrate, and ammonium concentrations for winter (December-January-February; filled circles) and summer (June-July-August; open circles). Also shown in panels **g-i** are the 1:1 lines, the correlation coefficients (r) between model and observations, and the corresponding reduced-major-axis regressions and slopes. $PM_{2.5}$ observations are from the China Ministry of Ecology and the Environment (MEE) national air quality monitoring network. OA and BC observations in Beijing, Handan, and Shanghai are from refs. [70-72]. Sulfate, nitrate, and ammonium observations are from the Campaign on Atmospheric Aerosol Research network of China (CARE-China)[36,48].

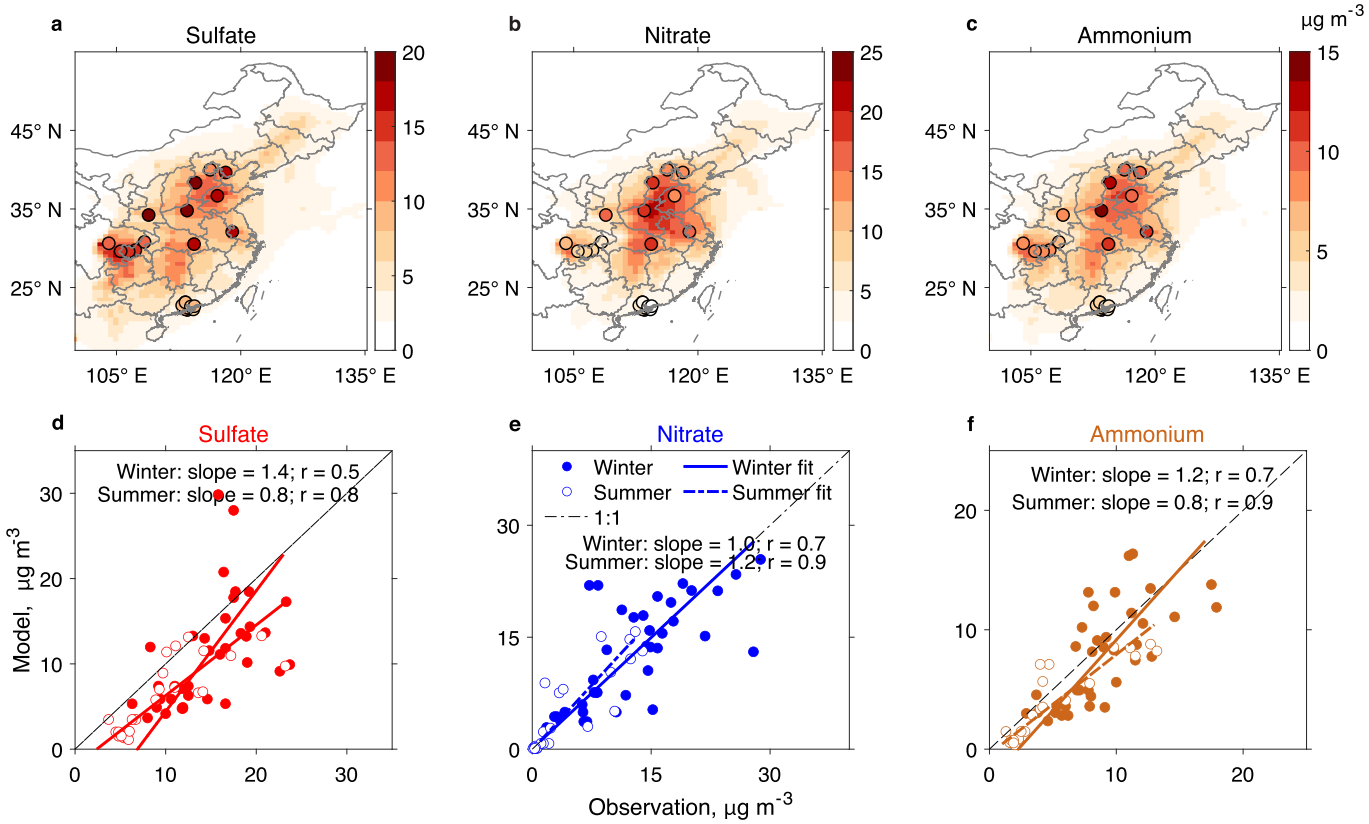

Extended Data Fig. 3 | Same as Extended Data Fig. 1 but for the year 2015 including January, February, July, and December. Observations are from ref. [37]. Here we only show sites that have both winter and summer observations, and summer observations for these sites are mostly for July.

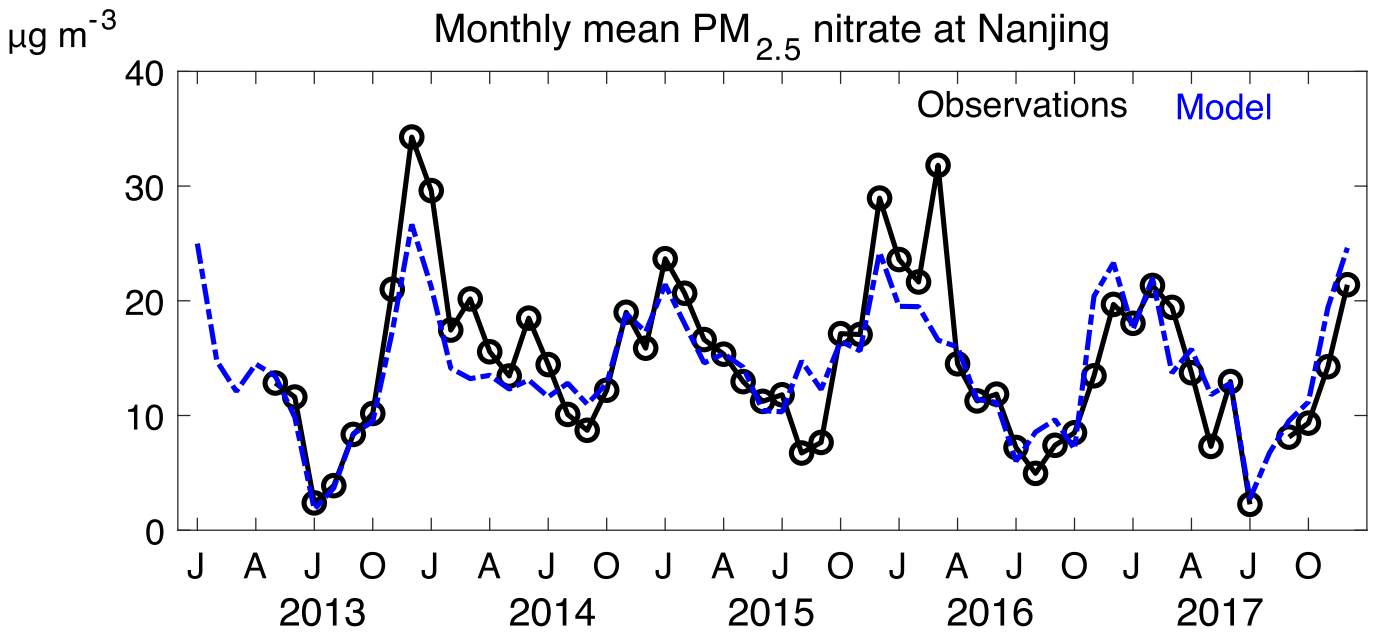

Extended Data Fig. 4 | Time series of monthly mean $PM_{2.5}$ nitrate at Nanjing from 2013 to 2017. GEOS-Chem results (blue dotted lines) are compared to observations (black solid lines). Observations are from the Station for Observing Regional Processes of the Earth System (SORPES; 118.97° E, 32.1° N) in Nanjing, and are detected by the Monitor for AeRosols and GAses in Ambient air (MARGA; Metrohm, Switzerland)[3,73]. The abnormally low nitrate in summer 2013 is mainly due to meteorological influence (Supplementary Fig. 3).

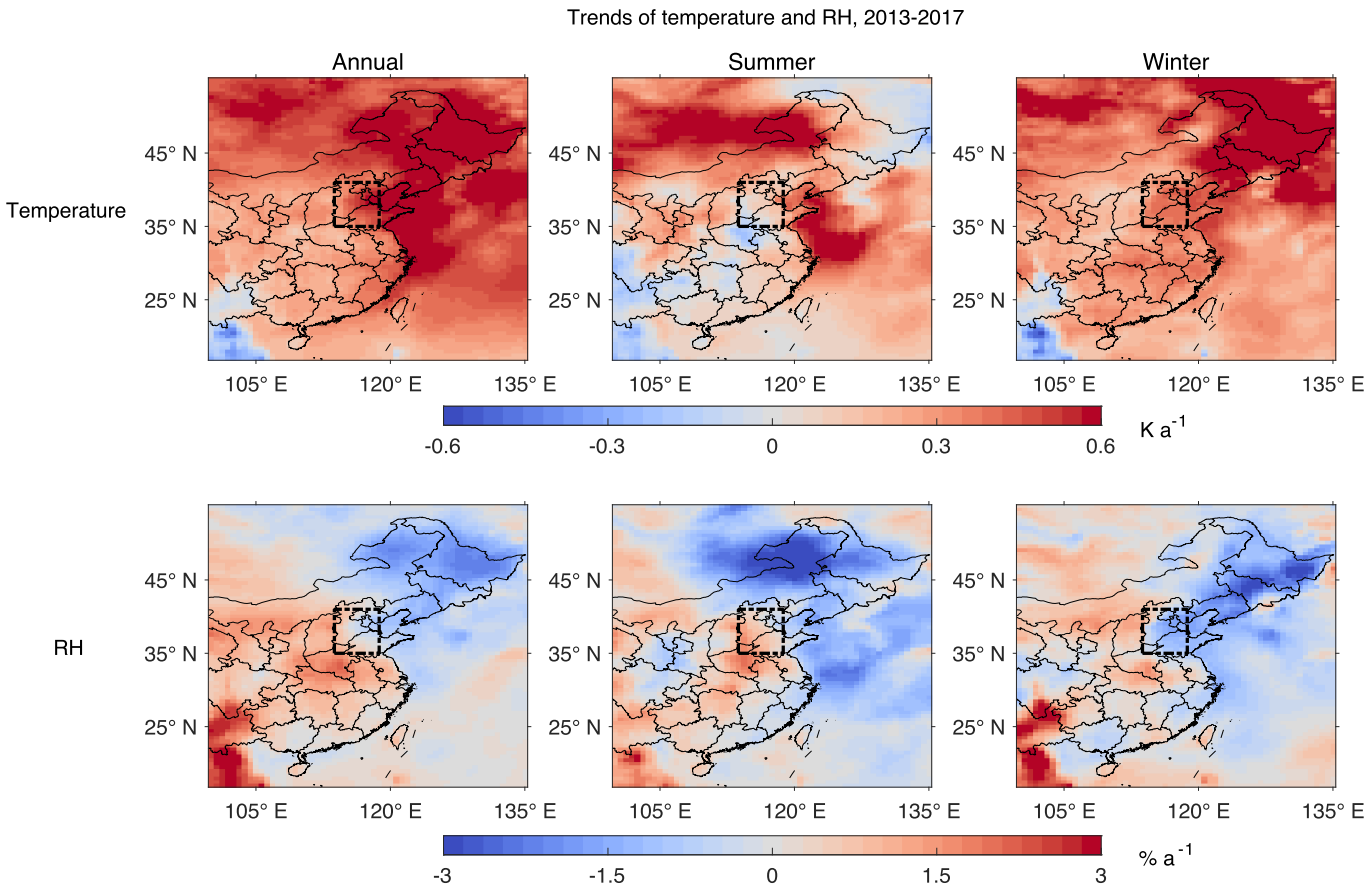

Extended Data Fig. 5 | Linear regression trends of temperature and RH from 2013 to 2017 for annual mean, summer, and winter conditions. Temperature and RH are from the MERRA-2 reanalysis data from the NASA Goddard Earth Sciences (GES) Data and Information Services Center (https://gmao.gsfc.nasa.gov/reanalysis/MERRA-2/data_access/). The dashed rectangles define the North China Plain region (113.75°-118.75° E, 35°-41° N).

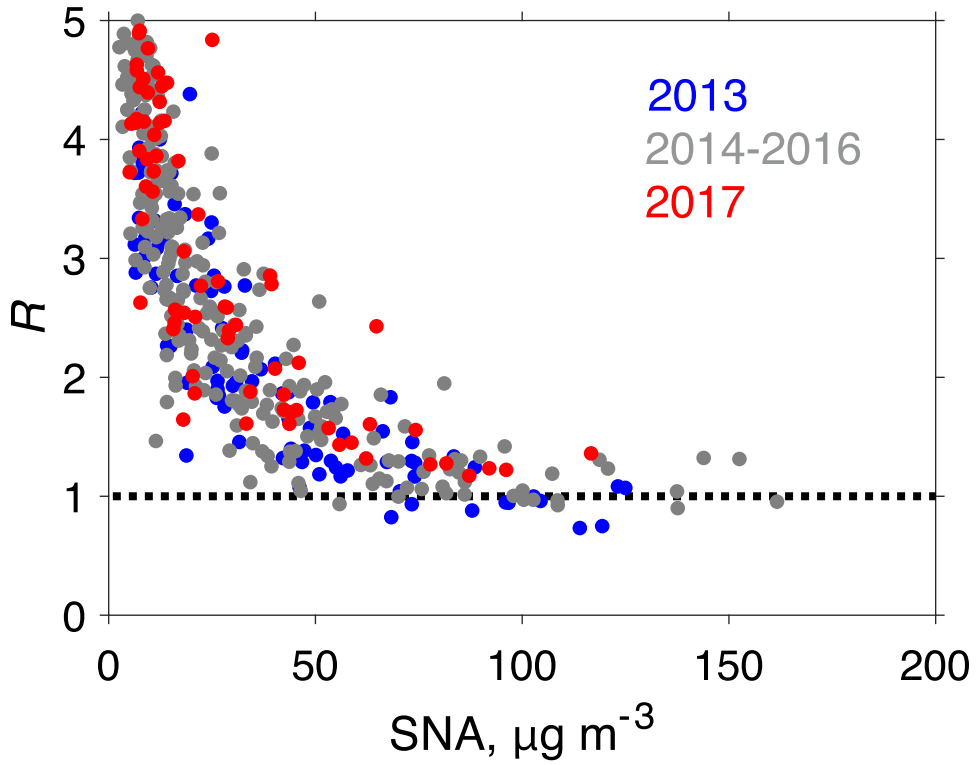

Extended Data Fig. 6 | Thermodynamic regime for ammonium nitrate particulate formation in the North China Plain in winter. The figure shows the molar ratio $R = [NH_3^T] / (2 \times [SO_4^{2-}] + [NO_3^T])$ as a function of sulfate-nitrate-ammonium (SNA) $PM_{2.5}$ concentrations in daily mean GEOS-Chem results for the North China Plain in winters 2013-2017. Formation of nitrate $PM_{2.5}$ is nitrate-limited if $R > 1$ (ammonia in excess) and ammonia-limited if $R < 1$ (nitrate in excess). The black dashed line indicates $R = 1$. This figure can be compared to Fig. 4a from ref. [44] which showed the same plot for observations in Beijing in December 2015 and December 2016. Bisulfate (HSO_4^-) in acid particles would modify the acid-base balance but we find from ISORROPIA II calculations that it accounts for less than 5% of total sulfate in the model, consistent with wintertime Beijing observations[44].

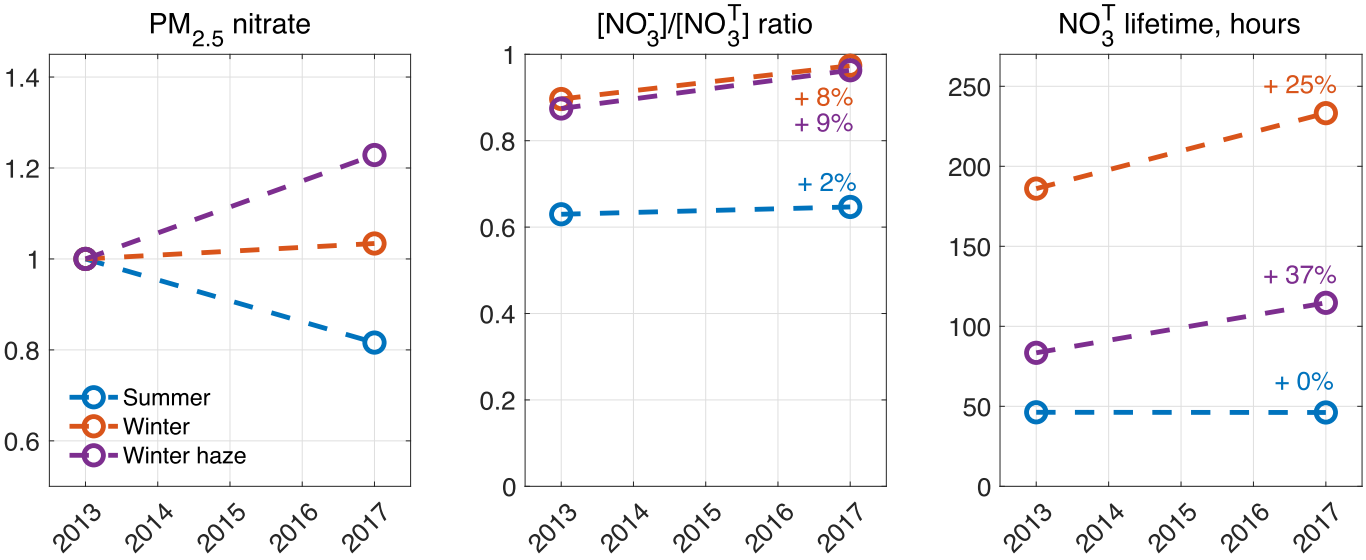

Extended Data Fig. 7 | 2013-2017 trends of $PM_{2.5}$ nitrate, the particulate fraction of total nitrate ($[NO_3^-]/[NO_3^T]$ molar ratio), and NO_3^T lifetime against deposition simulated by GEOS-Chem without implementation of the new wet deposition scheme in ref. [34]. Results are from GEOS-Chem driven by 2013 and 2017 MEIC emissions with 2017 meteorology applied to the two years.

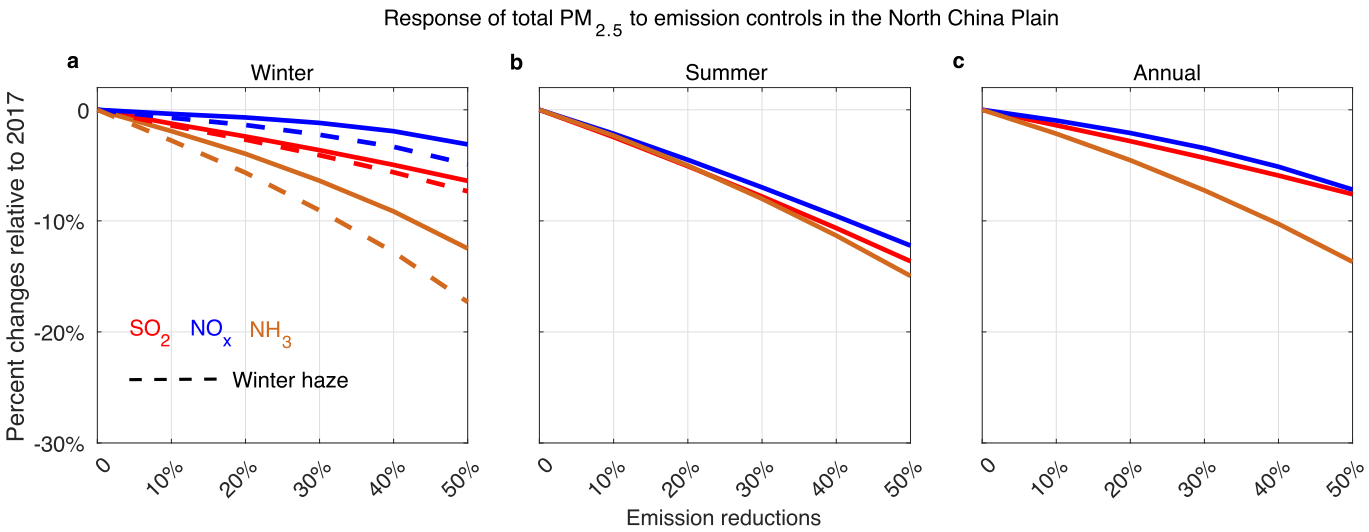

Extended Data Fig. 8 | Similar to Fig. 5 in the main text but for percent changes of mean total $PM_{2.5}$ in response to emission reductions averaged over the North China Plain relative to 2017.